

Quantized Hall resistance in large-scale monolayer graphene

Yanfei Yang¹, Chiashain Chuang^{1,2}, Chieh-Wen Liu^{1,3} and Randolph E. Elmquist¹

¹ National Institute of Standards and Technology, Gaithersburg MD, 20899 USA; ² Department of Physics, National Taiwan University, Taipei 106, Taiwan; ³ Graduate Institute of Applied Physics, National Taiwan University, Taipei 106, Taiwan

E-mail: Elmquist@nist.gov

Abstract: Graphene is a one-atom-thick carbon lattice that can be exfoliated from solid graphite or grown using high temperature processing methods on a variety of substrates. Many practical applications of large-area graphene, however, are limited by the transport mobility and carrier concentration homogeneity over distances greater than hundreds of microns. This presentation reports on the characteristics of large area (5 mm² to 25 mm²) monolayer devices that display precise quantum Hall effect (QHE) characteristics at reasonable cryogenic temperatures, surpassing the previously reported records for graphene.

Keywords: quantum Hall effect, graphene, electronic mobility, resistance standard

1. INTRODUCTION

Epitaxial graphene (EG) [1,2] is formed when silicon (Si) sublimates at high temperature on the surface of SiC(0001), a hexagonal crystalline material with a wide band gap. [3] The EG samples grown in our laboratory are annealed facing a glassy graphite disk. The role of vapor-phase byproducts (Si, Si₂C and SiC₂) is increased due to the geometrical arrangement of the substrate and confining graphite surface. [4] The result is a uniform EG monolayer over a large area, while bilayer graphene is suppressed and sometimes absent at millimeter scale.

We find that face-to-graphite (FTG) growth [5] in Ar background gas halts at one monolayer over most of the surface at temperatures up to 2000 °C. The optical images in figure 1(a,b) show two samples processed concurrently at 1950 °C (1800 s). Note that only ≈ 100 μm of the

surface near the edge of the FTG sample (figure 1a) has dark graphite filling the etched pits, while the interior region of the FTG sample is much more uniform. This uniform appearance is in contrast to the sample processed open to Ar background gas (figure 1b), which has a disordered EG layer and dark graphite covering all of the pits. Raman microscopy, optical

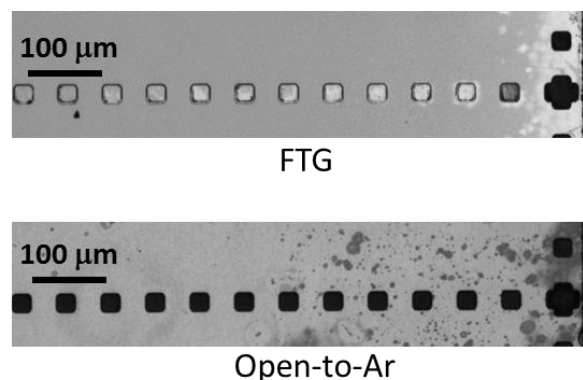


Figure 1. Optical microscope images showing the difference in EG near border regions of two samples processed together, (a) FTG and (b) open to Ar gas in the furnace.

images, atomic force microscopy (AFM), and electronic transport characteristics all show that the interior of FTG samples consists of uniform monolayer EG without appreciable inclusion of bilayer patches and with small atomic step heights.

2. FABRICATION AND SELECTION

Optically enhanced (OE) microscope imaging [6] makes visible the small ($\approx 2.3\%$) difference in transmission that occurs for light passing through a single layer of graphene, compared to the transmission through the insulating SiC substrate from which the EG has been removed. Figure 2 shows one large device that was processed at 1900°C (116 s), fabricated using a low-residue technique with a sacrificial 20 nm protective Pd/Au layer [7], photographed using OE microscopy, and measured using low-frequency ac magneto-transport. The images in the lower part of figure 2 show six regions of the sample near the Hall bar device with uniform OE contrast indicating homogeneous EG coverage. The two sets of magneto-transport characteristics shown in the upper part of figure 2 also indicate

that the EG is monolayer graphene, with uniform carrier concentration n . The values of resistivity $\rho_{xx} = (R_{Axx}/2 + R_{Bxx}/2) \times w/L$ were derived from the average resistance along both sides of the device and scaled by the ratio of width to length separating the potential terminals at the ends of region 1 and region 2.

Both regions of the device shown in figure 2 display similar transport characteristics with $R_{xy} \approx 12906.4 \Omega$ for magnetic field $B > 5 \text{ T}$ at temperature $T = 1.5 \text{ K}$. In the OE images, the main visible features are the SiC atomic terrace edges which appear as darker diagonal lines, and form at high temperature as the EG layer grows. Large terraces can be formed with atomic steps of height up to 10 nm, and these steps reduce the mobility by increasing the electronic scattering in EG [8]. We have found that for fixed carrier concentration n the mobility $\mu = \rho_{xx}(B=0)/ne$ is improved by reducing the height of extended terraces to $h < 3 \text{ nm}$. As the OE images of figure 2 scan progressively from left to right and are seen to be longer and more distinct, AFM shows that they increase in height. This coincides with

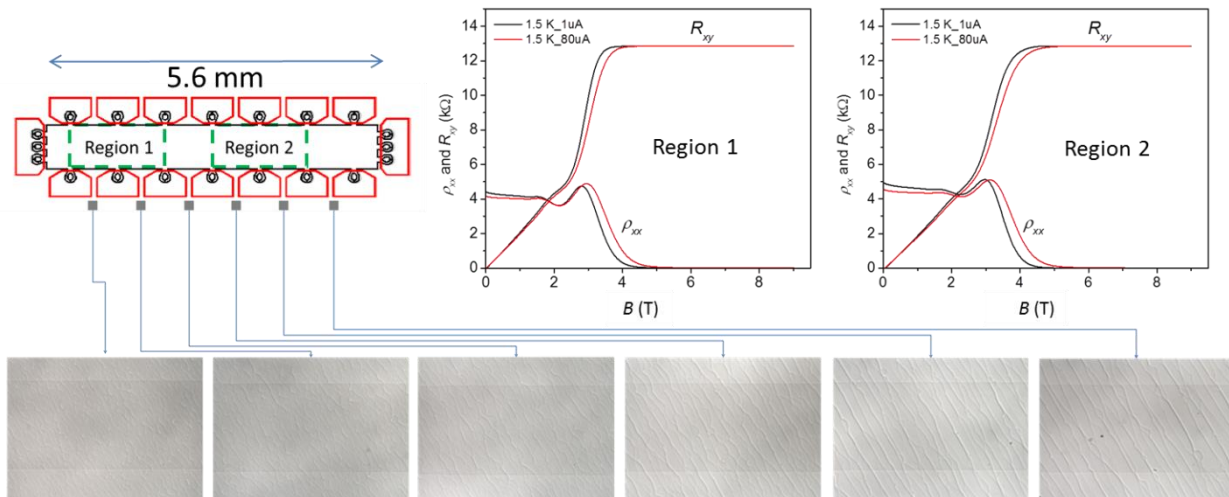


Figure 2. Design, magneto-transport characteristics, and OE images of a 5.6 mm long Hall bar device. The Hall bar channel is surrounded by multiple contacts so that the characteristics of different regions can be measured. Both region 1 and region 2 display excellent QHE plateaus, but the mobility of region 1 is 20 % higher as described in the text. This improvement corresponds to low and irregular terraces in the OE images at bottom, where EG is bordered at top and bottom by bare SiC.

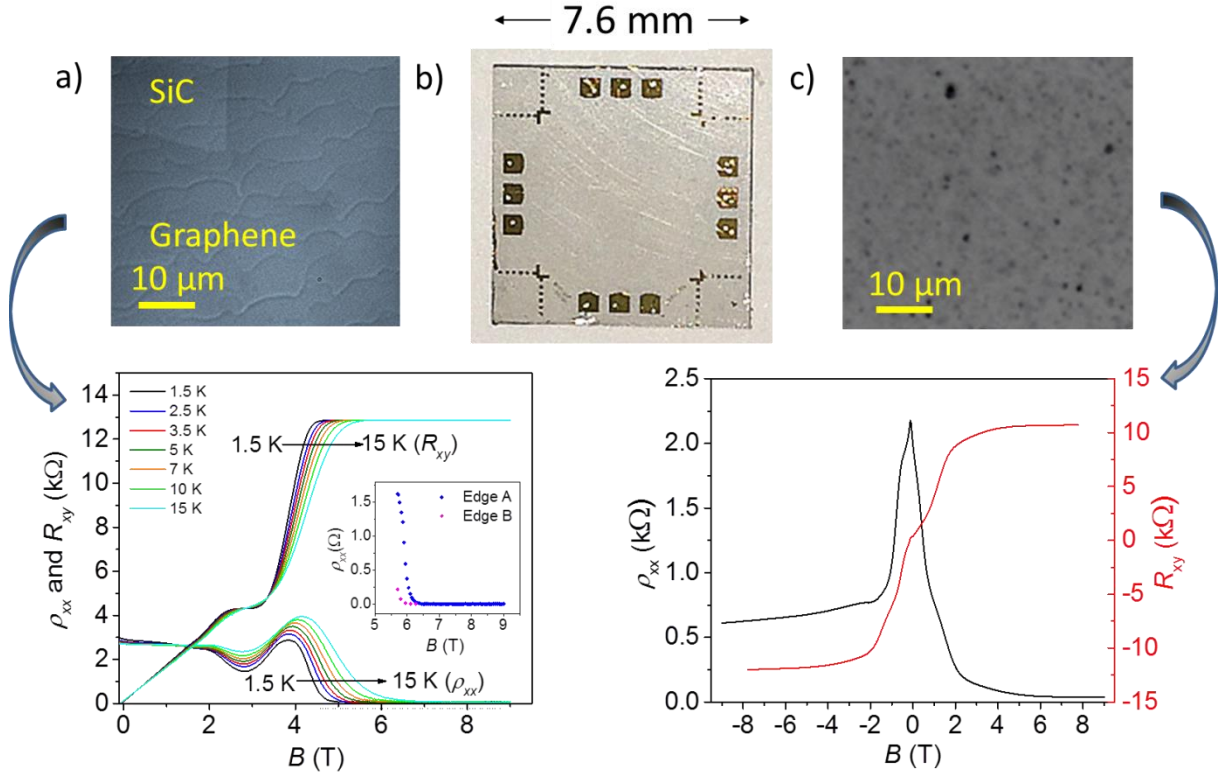


Figure 3. Large octagonal devices. The device shown in (a) and (b) was produced from FTG graphene, while the sample shown in (c) was annealed open to argon background gas. The QHE plateau is robust up to at least 15 K in the FTG sample, with full quantization above 7 T as shown in the inset. Only very weak QHE plateaus are observed for the other sample, with non-symmetric longitudinal resistivity for $\pm B$.

the reduction in mobility from $4600 \text{ cm}^2\text{V}^{-1}\text{s}^{-1}$ in region 1, to $3840 \text{ cm}^2\text{V}^{-1}\text{s}^{-1}$ in region 2.

3. CHARACTERIZATION

A robust quantum Hall effect has been observed in devices of octagonal shape as well as in the Hall bar configuration. Large octagonal samples were produced using both FTG and open-to-Ar graphene on SiC substrates. The FTG process clearly results in improved QHE properties in large samples when the EG is grown at $1900 \text{ }^\circ\text{C}$, as shown in figure 3. Figure 3a shows an OE image and gives the Hall resistance R_{xy} and longitudinal resistivity ρ_{xx} for one such large, octagonal device of size $5.6 \text{ mm} \times 5.6 \text{ mm}$. This device shows resistance plateaus for the Landau-level filling factors $\nu=6$ and $\nu=2$ above about

$B \approx 2.5 \text{ T}$ and 6 T , respectively, indicating a moderate level of carrier concentration ($n \approx 4 \times 10^{11} \text{ cm}^{-2}$), which is sufficient for the QHE $\nu=2$ plateau to be fully quantized. The device mobility is $5600 \text{ cm}^2\text{V}^{-1}\text{s}^{-1}$, due to low terrace steps and high-quality monolayer EG.

Although the wide sample geometry limits the resolution at low currents, the $\nu=2$ QHE plateau of this device between 7 T and 9 T gives longitudinal resistivity $\rho_{xx} = -150 \mu\Omega \pm 250 \mu\Omega$, or $\rho_{xx} < 10^{-8} \times R_{xy}$, when data was averaged over many measurements using a cryogenic current comparator bridge [9, 10] with dc source-drain currents $I_{SD} = \pm 74 \mu\text{A}$ and $T = 2.6 \text{ K}$. We will report these results as well as other precise QHE measurements showing that EG devices are suitable as quantized Hall resistance standards,

and possibly superior to most GaAs heterostructures now in use as resistance standards at many national laboratories.

4. DISCUSSION

Our results confirm and expand on many prior experiments showing that annealing SiC(0001) in confined Si vapor allows controllable EG growth. For the standards community, traceability from the QHE standard to 1 k Ω and 10 k Ω at current levels greater than 0.5 mA is within the capabilities of present-day room-temperature commercial resistance bridges, with relative uncertainty approaching 1×10^{-8} . Our results show promise for EG in studies of the frequency- and size-dependent electronic properties of graphene. Wafer-scale low-defect graphene also may lead to large-scale optical applications, high-frequency integrated circuits, optoelectronics and other useful applications.

5. REFERENCES

[1] Ruan M, Hu Y, Guo Z, Dong R, Palmer J, Hankinson J, Berger C and de Heer W, 2012 *MRS Bulletin* **37** 1138

[2] Forti S and Starke U 2014 *J. Phys. D: Appl. Phys.* **47** 094013

[3] Borovikov V and Zangwill A 2009 *Phys. Rev. B* **79** 245413

[4] Real M, Lass E, Liu F, Shen T, Jones G, Soons J, Newell D, Davydov A and Elmquist R 2013 *IEEE Trans. Instrum. Meas.* **62** 1454

[5] Camara N, Huntzinger J, Rius G, Tiberj A, Mestres N, Pérez-Murano F, Godignon P and Camassel J 2009 *Phys. Rev. B* **80** 125410

[6] Yager T, et al. 2013 *Nano Lett.* **13** 4217

[7] Yang Y, Huang L, Fukuyama Y, Liu F, Real M, Barbara P, Liang C, Newell D and Elmquist R 2015 *Small* **11** 90

[8] Ji S, Hannon J, Tromp R, Perebeinos V, Tersoff J and Ross F 2012 *Nature Mat.* **11** 114

[9] Bierzychudek M and Elmquist R 2009 *IEEE Trans. Instrum. Meas.* **58** 1170

[10] Hernandez-Marquez F, Bierzychudek M, Jones G and Elmquist R 2014 *Rev. Sci. Instrum.* **85** 044701